Title: A tool for predicting the thermal performance of a Diesel engine

Authors:

A.J. Torregrosa. Professor. atorreg@mot.upv.es

P. Olmeda. Associate professor. pabolgon@mot.upv.es

J. Martín. Assistant professor. jaimardi@mot.upv.es

C. Romero. On doctoral leave from Universidad Tecnológica de Pereira (Colombia). caromero@mot.upv.es

Addresses

CMT-Motores Térmicos

Camino de Vera s/n

46022 Valencia (Spain)

Tel: (+34) 96 387 76 50

Fax: (+34) 96 387 76 59

Corresponding Author:

Olmeda González, Pablo

CMT-Motores Térmicos

Camino de Vera s/n

46022 Valencia (Spain)

Tel: (+34) 96 387 76 50

Fax: (+34) 96 387 76 59

E-mail: pabolgon@mot.upv.es

Abstract.

This paper presents a thermal network model for the simulation of the transient response of diesel engines. The model was adjusted by using experimental data from a completely instrumented engine run under steady-state and transient conditions. Comparisons between measured and predicted material temperatures over a wide range of engine running conditions show a mean error of 7ºC. The model was then used to predict the thermal behavior of a different engine. Model results were checked against oil and coolant temperatures measured during engine warm-up at constant speed and load, and on a New European Driving Cycle. Results show that the model predicts these temperatures with a maximum error of 3ºC.

INTRODUCTION

The internal combustion engine (ICE) is currently facing two main problems: fuel consumption and exhaust emissions. These two factors are highly affected by the combustion process, which in turn is highly affected by heat transfer from the in-cylinder gases to the surrounding walls.

The description of heat transfer in ICE is a challenging task, considering the different systems (intake and exhaust ports, coolant circuit, lubricant oil subsystem), the different heat transfer mechanisms (convection, conduction and radiation), and the rapid and unsteady changes that take place inside the cylinder. Considerable experimental and theoretical efforts have been devoted over recent years in order to overcome these difficulties [1, 2].

Engine efficiency and pollutant emissions are highly affected by combustion chamber wall temperatures [3, 4]. Therefore, any strategies aiming at the control of these temperatures, which is usually accomplished through the coolant temperature control [5, 6], should be considered from early design stages [7].

The proper definition of the requirements for controlling the coolant temperaturemust be based on the detailed knowledge of engine thermal behavior, i.e., on the accurate prediction of material temperatures and heat flows through the engine elements.

In order to estimate properly these heat flows, it is necessary to combine theoretical studies with the analysis of experimental data. Regarding theoretical approaches, the use of simple lumped models has gained an increasing attention due to their reasonable compromise between computational cost and solution accuracy [8].

Shayler et al. [9] appear to have been the first to use this kind of models. However, in order to simplify the simulation they used the correlation proposed by Taylor and Toong [10], which does not take into account important parameters affecting heat rejection, such as exhaust gas recirculation or combustion chamber geometry. Bohac et al. [11] improved Shayler's approach by including Annand's model [12] for spark-ignition (SI) engines. The application of the same geometrical model to compression-ignition (CI) engines is questionable, mainly due to the differences in piston geometry: almost flat in SI engines, and with a bowl in CI engines.

Jarrier et al. [13] implemented and validated a nodal model for a medium-size engine at different operating conditions. The effort was focused on low loads (up to 50%) and medium speed (three-fourths of the rated speed) points, since the study was focused on the urban driving cycles of the New European Driving Cycle (NEDC). As serious shortcomings appear in the heat flux formulation introduced in the model, Charmantray et al. [14] included a model that takes into account the differences between the heat transfer coefficients in steady-state conditions and those in transient conditions. The main problem of that model lies in the fact that it was validated against a specific diesel engine, and no studies were performed on other engines in order to validate the approach. Another disadvantage is the rough discretization considered in the combustion chamber (only one node for the piston and the cylinder head, and two nodes for the cylinder), which appears to be very poor in view of the large temperature differences expected both in the piston [15, 16] and between the valves and the cylinder head material [8].

In order to overcome these lacks, a model with a higher spatial resolution, validated against two different engines, is proposed. This work is organized as follows: First, a brief description of the equivalent thermal circuit of the engine is given, with especial emphasis on the description of the combustion chamber. After that, the modeling of the different boundary conditions is described. Then a global view of the model code is provided, followed by the comparison between experimental and model results for a specially instrumented engine, in both stationary and transient conditions. Then the model is applied to a different engine in which coolant and oil temperatures are used for comparison. Finally, the main conclusions of this work are given.

ENGINE THERMAL MODEL

In the frame of the model considered, the engine is regarded as a thermal network consisting of a finite number of nodes, whose thermal inertia is characterized by a thermal capacitance, and linked to other nodes by means of thermal conductances. Once the structure is divided into nodes, the energy conservation equation can be written for each node. Figure 1 represents a node and all its possible interactions: conduction to other nodes, convection to a fluid, and heat sources. The energy balance on a node leads to:

$$m_i c_v \frac{T_{t+\Delta t}^i - T_t^i}{\Delta t} = \sum_j K_{ij}\left(T_{t+\Delta t}^j - T_{t+\Delta t}^i\right) + \sum_k q_{k\to i} + \sum_l h_{li} A_{li}\left(T_l - T_{t+\Delta t}^i\right) \qquad (1)$$

Here, m_i is the mass of node i , c_v its heat capacity, K_{ij} the conductance between nodes i and j , h_{li} the heat transfer coefficient between node i and a boundary l and A_{li} the corresponding contact area. The temperatures in the right-hand side are computed at time $t+\Delta t$ (implicit formulation) in order to ensure the stability of the calculation when considering transient processes.

Writing equation (1) for each of the nodes gives an implicit set of linear equations of the form:

$$\left(\mathbf{K}+\frac{1}{\Delta t}\mathbf{C}\right)\mathbf{T}_{t+\Delta t}=\mathbf{Q}+\frac{1}{\Delta t}\mathbf{C}\mathbf{T}_{t}+\mathbf{H} \tag{2}$$

where $\mathbf{T}_t$ and $\mathbf{T}_{t+\Delta t}$ are column n-vectors with the node temperatures at times t and t + Δt, respectively, $\mathbf{Q}$ is a column n-vector with the sum of the heat fluxes exchanged by each node (including, among others, a heat flux generated by friction), $\mathbf{H}$ is a column n-vector with the sum of the terms $T_l h_{li} A_{li}$ related to the convective boundary conditions associated with node i, and $\mathbf{K}$ and $\mathbf{C}$ are $n \times n$ conductance and capacitance matrices, respectively.

The diagonal elements of the conductance matrix are the sum of all the conductances connected to the corresponding node, whereas off-diagonal elements K_{ij} represent the conductance between nodes i and j with a minus sign. Conductive conductances are calculated accordingly to the geometry of the connection between nodes - planar ($k_{ij}A_{ij}/x_{ij}$) or radial ($2\pi k_{ij}l_{ij}/\ln(r_j/r_i)$ -, whereas convective conductances are computed as the product of the heat transfer coefficient and the contact area ($h_{ij}A_{ij}$). Thus, assuming that all conductances are linear one has.

$$\begin{aligned} K_{ij} &= \sum_j k_{ij}A_{ij}/x_{ij} + \sum_l h_{li}A_{li} \quad \text{if} \quad i=j \\ K_{ij} &= -k_{ij}A_{ij}/x_{ij} \;\; or \;\; K_{ij}=-h_{ij}A_{ij} \quad \text{if} \quad i\neq j \end{aligned} \tag{3}$$

In steady-state conditions, since $T^i_{t+\Delta t}=T^i_t$, Eq (2) reduces to

$$\mathbf{K}\mathbf{T}=\mathbf{Q}+\mathbf{H} \tag{4}$$

Either Eq. (2) or Eq. (4) is assembled automatically, based on general engine specifications, and solved implicitly for the temperature vector $\mathbf{T}$ by using a Gaussian elimination procedure.

Geometrical node division.

The node division was defined by using a real geometrical model of the engine (three-dimensional [3D] model). After that, the complex geometries were divided into small parts, considering both the Biot number criterion [17] and the position of the temperature sensors available, so that direct comparison between model and experimental results was allowed. Then the main characteristics of the nodes were calculated: mass, connecting areas, and distances between centers. These, together with the thermal characteristics of the material, allow for the calculation of the thermal resistor network (conductances and capacitances). The following discretization was used in this work:

- The liner was divided into three axial, three radial, and six circumferential levels, so that the cylinder liner was represented by 54 nodes (Figure 2).
- The piston was divided into six nodes, referered to, from top to bottom, as bowl centre, bowl rim, piston crown, piston centre, oil cooling gallery housing, and piston skirt (Figure 3).
- The cylinder head consists of the fire deck, the exhaust and intake runners, the valves with their guides and the injector. All these elements were separated into two different parts: lower and upper. The cylinder head model was divided into 35 nodes. (Figure 4).

With this discretization, the thermal resistor network consists of 95 metallic nodes. The boundary conditions were represented by five convective nodes (in-

cylinder gases, intake air, exhaust gases, coolant, and lubricating oil), characterized by their average temperatures and film coefficients.

Even though the heat fluxes through the combustion chamber walls change periodically with time, a steady state was assumed in the analysis, so that cycle averaged values were used. This assumption is reasonable considering the characteristic rate of the periodical changes as compared to the thermal inertia of the metallic parts of the cylinder head, piston, and liner [11]. The expected change in gas temperature can be higher than 700ºC, while changes of only 10–15ºC are expected in the material temperatures [18]. The same assumption is valid for the exhaust and intake gases. Of course, neither the thermal fatigue nor the peak temperatures due to the periodicity on the material temperatures can be identified with this approach.

The boundary conditions, i.e., the links between the convective nodes and the corresponding material nodes, were modelled as described in the following.

Interaction between in-cylinder gases and combustion chamber walls

As already mentioned, the mean wall temperatures, T_w, during the engine working cycle were predicted by using heat flows calculated from cycle averaged values. The mean heat flux $\overline{Q}$ between the gas and a wall is calculated as:

$$\overline{Q} = \frac{1}{720}\int_0^{720} Q(\alpha)\,\mathrm{d}\,\alpha = \frac{1}{720}\int_0^{720} h_g(\alpha)A(\alpha)\left[T_g(\alpha) - T_w(\alpha)\right]\mathrm{d}\,\alpha \qquad (5)$$

Here $h_g(\alpha)$ is the instantaneous heat transfer coefficient and $T_g(\alpha)$ the instantaneous gas temperature, as a function of the crank angle α.

Considering that the wall temperature can be considered constant over the thermodynamic cycle, this mean heat flux can be also expressed as:

$$\overline{Q} = \overline{h_g A}\left(\overline{T_g} - T_w\right) \tag{6}$$

Where the mean values are defined as:

$$\overline{h_g A} = \frac{1}{720}\int_0^{720} h_g(\alpha) A_g(\alpha)\,\mathrm{d}\alpha \tag{7}$$

$$\overline{T_g} = \frac{1}{\overline{h_g A}}\frac{1}{720}\int_0^{720} T_s(\alpha) h_g(\alpha) A_g(\alpha)\,\mathrm{d}\alpha \tag{8}$$

If the wall is permanently in contact with the gas, i.e., the contact area does not change with crank angle, Eqs. (7) and (8) can be simplified.

The conductance between the in-cylinder gases and the internal nodes of the cylinder liner was calculated taking into account that they are not in contact during the whole cycle (Figure 5), so that the contact area depends on the crank angle and on the node considered, and therefore different gas temperatures are used as boundary conditions for different nodes.

The film coefficient h_g necessary to calculate all the conductances between the in-cylinder gases and the surrounding walls was obtained by using an enhanced version of the Woschni equation [19], which is one of the most broadly used correlations in diesel engines. This correlation lacks a specific term representing radiation, which is, however, taken into account through the so-called combustion term, i.e., the last part of Eq. (9) [19]:

$$h_g = 1.2\times10^{-2} D^{-0.2} p^{0.8} T_g^{-0.53}\left[(b_1 c_m + b_2 c_u) + b_3\left(\frac{V_T T_{IC}}{p_{IC} V_{IC}}\right)(p - p_0)\right]^{0.8} \tag{9}$$

Here, the instantaneous gas temperature is calculated with the measured in-cylinder pressure p assuming perfect gas behavior; c_m is the mean piston speed; c_u is the tangential velocity at the cylinder wall due to swirl; V_T is the total displacement; T_{IC}, p_{IC} and V_{IC} represent the gas temperature, pressure, and

cylinder volume at intake valve closing (IC), respectively; and p_0 is the in-cylinder pressure under motoring conditions.

Runner – gas heat transfer

The heat transfer between the runners and the gas is highly unsteady (especially in the exhaust, where very high gas velocities are reached during the blow down). Since the generated turbulence lasts even after valve closing, expressions based on the instantaneous flow velocity do not properly describe the heat transfer in this pulsating flow. Therefore, a different approach was considered, based on the recursive calculation of an average velocity, $\bar{c}_{g,ru}(t)$, as [20]

$$\bar{c}_{g,ru}(t) = b_4 \bar{c}_{g,ru}(t-\Delta t) + (1-b_4) c_{g,ru}(t) \tag{10}$$

where $c_{g,ru}(t)$ is the actual velocity and b_4 is a suitable weighting factor related to the flow unsteadiness. This average speed was used to calculate the Reynolds and Nusselt numbers as

$$\overline{\mathrm{Re}} = \frac{c_{g,ru}\phi_{ru}}{\nu_g} \tag{11}$$

$$\mathrm{Nu} = 1.6\overline{\mathrm{Re}}^{0.4} \tag{12}$$

The instantaneous velocity was obtained from a combustion diagnostics code [21]. The intake and exhaust gas temperatures and heat transfer coefficients, obtained from the Nusselt number, were averaged over a cycle in a way similar to that used for the in-cylinder mean film coefficient and the apparent gas temperature.

Coolant – wall heat transfer

The heat transfer coefficients between the coolant and the liner and between the coolant and the head were calculated taking into account the coolant flow by means of a modified Dittus–Boelter correlation [22], since forced convection is the dominant regime in these systems:

$$\mathrm{Nu} = 0.023\,\mathrm{Re}_{\phi}^{0.8}\,\mathrm{Pr}^{0.4} \tag{20}$$

Although the previous correlation was developed for straight pipes, it has been demonstrated to be useful for this application [23].

Oil - walls.

The piston is cooled in two different ways: Part of the heat is transmitted through the segments to the liner and finally to the coolant. Most of it, though, is transferred to the oil. In the engine under study, the oil is sprayed to the entrance of a gallery in the piston crown with an oil cooling jet. In order to find the heat transfer coefficient, an expression based on boundary-layer theory was used [24–26]:

$$\mathrm{Nu}_{gal} \propto \mathrm{Re}_{gal}^{b_5}\,\mathrm{Pr}^{b_6} \tag{1}$$

Since variations on Prandtl number were small for the measured temperature ranges, a correlation for the conductance between the oil and the piston was determined in the following way:

$$K_{pis-oil} = b_7 c_m^{b_5} \tag{2}$$

Both constants, b_5 and b_7, were adjusted by means of an optimization routine [8].

Regarding the cylinder liner, oil is continuously splashed against the cylinder wall, and in the piston some channels coming from the cooling gallery feed the third ring groove. Therefore, the cylinder wall is continuously wetted with oil. This oil is heated by the cylinder wall and scrapped-off during the downward

stroke. For this conductance, piston speed dependence was taken into account just as for the oil-piston heat transfer, but during the adjustment this dependence was found to be non-significant, whence only the constant part, denoted as $h_{lin-oil}$, was included.

Additionally to the convective interactions just described, there are three conductive conductances that cannot be obtained directly from the geometry: Piston - cylinder liner, cylinder head - cylinder liner and valve - valve seats. These interactions were treated as follows:

- In the first case (piston-cylinder liner), an empirical model was fitted to the temperatures measured in the piston and the liner. The conductance between a node of the piston and a node in the liner, which have contact through a piston ring, is given by:

$$\mathrm{K}_{pis\text{-}lin} = \frac{t_{con}}{t_{cycle}} K_s \beta_j \frac{D}{2} \qquad (3)$$

  Here it was assumed that the ring conductance per unit length, K_s, was constant since it was found that the influence of piston speed was not significant; t_{con} is the contact time between the segment and the liner node, t_{cycle} is the duration of a cycle, β_j is the angular width of the liner node and D *is* the bore. The contact time is calculated from the instantaneous piston position, taking into account both the position of the ring and the axial position of the liner node.
- The heat transfer between the cylinder head and the liner was neglected, since the gasket was made of a perforated metallic core coated with synthetic rubber on both sides, whose conductivity is very low compared

to the conductivities of other materials in the system, so that it could be considered as adiabatic [27].

- The conductance between the valves and their seats is the product of the valve seat area times a contact conductance, K_{seat} (which accounts for the contact time between valve and seat): $K_{valve-head} = A_{seat} K_{seat}$. For the contact resistance K_{seat} a value of 3 000 W/m^{2}K was used [17].

COMPUTATIONAL PROGRAM.

The main structure of the program is shown in Figure 6. This structure provides high flexibility; for instance, the user can define the number of nodes just by changing the input, defining the engine discretization, so that the placement of the thermocouples do not necessarily coincide with the mass centres of the nodes.

The program can be used in two modes: prediction or adjustment. In the predictive mode, temperatures and heat fluxes are calculated, whereas in the adjustment mode the model parameters are adjusted by using a Nelder-Mead simplex algorithm based separately on the root mean square (RMS) error of the mean temperatures of piston, fire deck and liner. The mean of these three errors gives the test error, while the mean of all the test errors gives the model error as:

$$\varepsilon_m = \frac{1}{N_{tests}} \sum_{N_{tests}} \left(\frac{1}{3} \sum_{pis,head,lin} \sqrt{\frac{\sum \left(T_{meas} - T_{pred} \right)^2}{N_{TC,i}}} \right) \qquad (4)$$

Here, T_{meas} is a measured temperature, T_{pred} is the predicted temperature, $N_{TC,i}$ is the number of temperature measurements in the piston, the head or the liner, and N_{tests} is the number of tests used to adjust the model.

RESULTS AND DISCUSSION.

The experimental work comprised the following steps:

- First, the model was adjusted and validated by comparing the modeled and measured results for the baseline engine.
- Next, the adjusted model was used to predict the transient behaviour of the baseline engine.
- Finally, the model was used to analyze the thermal performance of a second different engine, tested under both constant load (50 Nm at 1500 rpm) and urban driving transient cycle (NEDC). For this engine, coolant and oil temperatures were measured together with two external thermocouples attached to the cylinder head. Additionally, mean parameters and instantaneous in-cylinder pressures were recorded for a number of steady-state points extracted from the driving cycle.

Model setup and validation.

Extensive experimental work on a four-cylinder Diesel engine was performed for model adjustment and validation. The originality of the work lies on the fact that one of the engine cylinders was completely isolated from the other three, i.e., the injection, intake and exhaust systems were duplicated and controlled independently while keeping the four cylinder configuration. Additionally, the isolated cylinder was duly instrumented with 23 thermocouples in the cylinder liner, 16 thermocouples in the cylinder head, and 2 thermocouples in the piston (a detailed description of the set-up can be found in [28]). The main characteristics of this engine are given in Table 1.

The parameters of the model were adjusted by comparing its output with measurements performed along a set of tests in which speed, load (mean

effective pressure, bmep), manifold intake pressure, oil temperature and coolant temperature were varied. Table 2 gives an overview of the tests used to adjust the parameters of the model, while the adjustment results are shown in Table 3. At this point, it should be remarked that while these results are suitable for this particular engine, they may change from one engine to another.

Figure 7 shows comparisons between the predicted and measured liner temperatures at several axial locations for three different operating points. The model results predict reasonably the trends observed in the measurements. Additionally, a temperature gradient from the top to the bottom of the liner is observed, which is more obvious in the upper part of the liner (the refrigerated part) than at the lower part. In general, the model predicts properly the liner temperatures, but noticeable discrepancies between measured and predicted values are observed in the liner nodes located between the cylinders (Figure 7a). Two main reasons may explain this: on one hand, the use of a global spaced averaged heat transfer coefficient for the coolant-liner interaction; on the other hand, the heat flux coming from the adjacent cylinder, not accounted for in the model. Finally, an increase in temperatures with load and speed is observed, as expected. The load increase produces a higher gradient in the upper part of the liner, while the speed increase produces a more uniform temperature distribution along the stroke.

In Figure 8, comparison is given between predicted and measured temperatures in those liner nodes closest to the combustion chamber (at a depth of 8 mm). The maximum discrepancies are observed again in the node between cylinders, for the same reasons given earlier, but the mean error on liner prediction is 3.9 ºC.

As mentioned earlier, the cylinder head was divided into an upper and a lower part, with the latter being in contact with the in-cylinder gases, so that heat is transmitted from this part to the upper part and to the coolant. Figure 9 shows a comparison between temperatures measured and predicted for nodes located at the lower part of the cylinder head. The temperatures of these nodes were measured at a depth of 3.5 mm, except in the case of the injector hole, where the sensor was placed at a distance of 8.7 mm from the combustion chamber wall. The mean error in the predicted temperatures is 7.5 ºC, being lower at low loads, which are the dominant running conditions in the NEDC cycle.

The piston was divided into six nodes, but only the temperatures at two locations (bowl rim and bowl bottom) were available. The predicted and measured temperatures for these two nodes are compared in Figure 10, showing acceptable agreement between measured and predicted values for the bowl rim and some overprediction (with an average error of 15 ºC) for the bowl bottom, which is the largest error in the model. This is due to both the small number of sensors available and the fact that piston is the engine component with the highest number of interactions to be adjusted. Nevertheless, the mean error in piston temperatures is about 10ºC.

The average error, taking into account the liner, cylinder head and piston errors, is just 7.4 ºC, which can be regarded as acceptable, considering that a 50 ºC wall temperature change has a 1% effect on the estimate of the total heat released. Additionally, an error of 10% in in-cylinder heat transfer leads to an error of the order of 1% in engine performance, whereas a deviation of 7% in this heat transfer does not affect the in-cylinder gas pressure [29].

Once the model was validated, the heat fluxes could be analyzed. In Figure 11 the heat fluxes on a steady-state engine condition are shown. In this particular condition:

- The heat from in-cylinder gases is transferred to the piston (42 %), to the cylinder head (32 %) and to the liner (26 %). In the case of the liner, almost 50 % of the heat is transferred to the upper part, due to its longer contact time with the combustion gases.
- The heat received by the piston is transmitted by two paths: to the liner through the piston rings (16 %) and to the coolant oil (84 %). Finally, heat is transferred from the oil to the coolant.
- In the case of the liner, heat comes from combustion gases and from the piston (through the piston rings). This heat is then transferred to the coolant, either in a direct way (51 %) or through the coolant oil (49 %).
- Finally, the cylinder head receives heat both from the combustion chamber gases (63 %) and from the exhaust gases (36 %). This heat is transferred to the intake air (2%) and to the coolant (98 %).

Summarizing, the heat received by the coolant comes directly from the cylinder head (42 %) and from the liner (16 %), and indirectly from the piston and the cylinder liner through the lubricant oil (42 %).

Such a heat balance can be performed for each operating point, making the model suitable for the analysis of engine cooling systems at any given running condition.

Engine modeling under transient conditions.

In a second step, the model was used to analyze the thermal response of the engine under transient conditions, regarding transient operation as a process

between two steady-state operation points. In this way, the model uses the initial and final conditions, in each calculation step, in order to calculate the temperature evolution and hence the thermal fluxes. An interpolation procedure, in the time domain, allows for the comparison of the predicted and experimental transient thermal responses of the engine.

In order to model engine warm-up, mean variables and instantaneous values for in-cylinder gases were recorded at different steady state conditions. It was assumed that during the transition period, the averaged bmep and the instantaneous in-cylinder pressure are identical for steady and unsteady operations. In fact, bmep is affected during the warm-up by the friction mean effective pressure, which depends on the oil viscosity (temperature dependent).

It was also assumed that, due to the rate at which in-cylinder processes take place, the cycle-averaged heat transfer coefficient and temperature were still valid for warm-up transient conditions. A significant number of complete thermodynamic gas cycles can take place prior to the engine being noticeably affected by transient thermal conditions resulting from a change in engine operating conditions [30].

In this procedure, a time-step length of 1 s was used as a compromise between computational efficiency and prediction accuracy. The experimental measurements, consisting of 26 different transient processes, are summarized in Table 4. For these tests, piston temperature measurements were not available.

Figure 12 shows the temperature evolution of two extreme longitudinal locations of the cylinder liner (8.8 mm and 89.1 mm away from the fire deck), along two transient tests:

- From 2.4 bar bmep to 8.8 bar bmep at 4500 rpm,
- From 3.3 bar bmep to 10.7 bar bmep at 1000 rpm.

It seems that the model slightly overpredicts the temperature evolution of the nodes. This is caused, on one hand, by the quasi-steady approach used and, on the other hand, by the node discretization used in the longitudinal dimension of the liner (this is not actually a constraint for the model), which determines the accuracy of temperature resolution. Obviously, a refinement of the cylinder mesh would determine properly the time constants, but at the expense of an increase in the computational cost.

In the case of the fire deck nodes, transient results are presented in Figures 13 and 14, where the predicted thermal response follows reasonably the experimental trends, so that it can be considered that the corresponding time constants were acceptably modelled. Of course, as the engine transient thermal process is a complex multi-order dynamic process, it cannot be simplified to a first order dynamic process for any of the operation points; however, the time constant may be a useful approach for a qualitative evaluation. Finally, the predicted piston response is plotted in Figure 15, where the faster evolution of the piston rim when compared to the piston bottom is due to its lower heat capacity.

In some nodes, transient predictions exhibit large deviations with respect to the experimental results. These deviations are associated both with the uncertainties in the engine transient thermal phenomena (for instance, the friction model) and with the model simplifications (finite number of nodes, simplified heat transfer correlations, etc.). In general, the model provides

satisfactory insight into the evolution of temperatures and heat fluxes during engine transient operation.

In Figure 16 prediction of both heat fluxes and mean combustion chamber temperatures are shown when the engine is subject to a random driving cycle consisting of a set of validated transitional processes. It can be observed that the transient heat flow through the combustion chamber walls stabilizes very rapidly (the combustion process may take from 0.2 to 1.5 seconds to reach its steady state condition). For the transition regimes, the time constants for the engine nodes are of 35-65 s on average, neglecting the time taken for the combustion process to reach its steady-state condition, which is small compared with this elapsed time.

Modeling and validation of a similar engine through warm-up.

In order to check the validity of the conductances adjusted for the first engine, they were used on a second engine (Table 5 shows its main characteristics). This engine was tested under a set of steady-state running conditions and during different warm-up evolutions (constant torque and speed and driving cycles):

- The steady-state tests were mainly used to obtain input parameters for the model, i.e., in-cylinder pressure and temperature and mean variables.
- The warm-up tests were used to compare predicted and measured temperatures (coolant, oil and two cylinder head surfaces) in order to validate the model as a general model, valid not only for the first engine but for any transient study.

In this second engine, material temperature measurements were not available (except for the external surface of the block), and thus validation was carried out by comparing oil and coolant temperature evolutions (modelled and measured). Figure 17 shows the evolution of these temperatures for a warm-up process (50 Nm - 1500 rpm). Both predicted fluid temperatures follow the same trends as the experimental ones. Additionally, the maximum differences are of 2 ºC for the coolant and of 1.5 ºC for the oil. These results are satisfactory and lead to the conclusion that the internal temperatures of the material were reasonably predicted, since they were used as a boundary condition for the calculation of fluid temperatures. Moreover, the measured external block temperature follows the same trend.

Finally, the viability of using the thermal model on a specific transient evolution was checked. The profile chosen was the New European Driving Cycle (NEDC) which consists of four consecutive urban driving cycles (UDC), followed by an extra urban driving cycle (EUDC). Figure 18 shows a comparison between experimental and modelled results for coolant and oil temperatures along this cycle. Average predicted temperatures for the cylinder head, the liner and the piston are also presented in Figure 19, where the shapes of the curves keep the expected trends and magnitudes, relative to the actual evolution of coolant and oil temperatures, taken as a reference.

CONCLUSIONS.

An extension of a three-node concise wall temperature model based on a lumped method has been performed and evaluated. The new model was validated using experimental data from both steady state and transient thermal conditions. Global measurements of engine variables from the test bench, along

with instantaneous values of in-cylinder gas properties, effective valve sections, flows, and local temperature measurements in the engine solid masses, coolant and oil, were used during the development process. The updated model allows for a higher degree of discretization, and it provides local and global heat flows and temperature field information. These can be used as a boundary condition in engine cooling system models or combustion prediction and diagnosis models.

The predictive capability of the model was checked in two different engines. The first one was used as a reference engine, due to its temperature instrumentation, and a comparison between measured and calculated metal temperatures was performed in both steady state and transient tests. In the second engine, the comparison was performed on fluid (coolant and oil) temperature evolution in transient processes (warm-up and homologation cycle), since the metal temperatures were not available.

The next phase of the on-going research is to couple the model presented with an engine cooling subsystem model. This will allow studying the impact of different cooling strategies on oil, coolant and metal temperatures. Further work with the program comprises a more detailed calibration of the engine model, introducing friction model data from an engine of known dimensions and masses.

ACKNOWLEDGMENTS

The authors want to thank A. Guzmán for his valuable assistance in the experimental tasks and the Reviewers for their interesting comments.

NOMENCLATURE

A	Area	m^{-2}

b	Weighting factors	-
bmep	Brake mean effective pressure	bar
c	Speed	$m\ s^{-1}$
c_v	Heat capacity	$J\ kg^{-1}\ K^{-1}$
C	Capacitance	$J\ K^{-1}$
d	Distance	m
D	Bore	m
h	Heat transfer coefficient	$W\ m^{-2}\ K^{-1}$
H	Heat convection vector	-
k	Conductivity	$W\ m^{-1}K^{-1}$
K	Conductance	$W\ K^{-1}$
l	Length	m
m	Mass	kg
N	Number of tests	-
Nu	Nusselt number	-
p	Pressure	Pa
Pr	Prandtl number	-
Q	Heat flux	W
r	Radius	m
Re	Reynolds number	-
t	Time	s
T	Temperature	K
V	Volume	m^3
V_T	Total displacement	m^3

Greek symbols

α	Crank angle	º
β	angular width	
ε	Root mean square error	-
ϕ	Diameter	m
ν	Viscosity	$m^2\ s^{-1}$

Subscripts

0	Motored conditions
con	Contact
g	gas
gal	gallery
i,j,k,l	Node number
IC	Intake valve closing
lin	Liner
m	Mean
meas	Measured
pred	Predicted
pis	Piston
ru	Runner
s	Segment
u	Tangential
t	time
w	Wall

Superscripts

i,j,k,l	Node number

REFERENCES

[1] Borman, G., and Nishiwaki, K., A Review of Internal Combustion Engine Heat Transfer, Progress in Energy and Combustion Science, vol. 13, pp. 1–46, 1986.

[2] Finol, C. A., and Robinson, K., Thermal Modeling of Modern Engines: A Review of Empirical Correlations to Estimate the In-Cylinder Heat Transfer Coefficient, Proceedings of the Institution of Mechanical Engineers Part D–Journal of Automobile Engineering, vol. 220, no. 12, pp. 1765–1781, 2006.

[3] Broatch, A., Luján, J. M., Ruiz, S., and Olmeda, P., Measurement of Hydrocarbon and Carbon Monoxide Emissions During the Starting of Automotive DI Diesel Engines, International Journal of Automotive Technology, vol. 9, no. 2, pp. 129–140, 2008.

[4] Torregrosa, A. J.,Olmeda, P.,Mart´ın, J., and Degrauwe, B., Experiments on the Influence of Inlet Charge and Coolant Temperature on Performance and Emissions of a DI Diesel Engine, Experimental Thermal and Fluid Science, vol. 30, no. 7, pp. 633–641, 2006.

[5] Pang, H. H., and Brace, C. J., Review of Engine Cooling Technologies for Modern Engines, Proceedings of the Institution of Mechanical Engineers Part D-Journal of Automobile Engineering, vol. 218, no. 11, pp. 1209–1215, 2004.

[6] Torregrosa, A. J., Broatch, A., Olmeda, P., and Romero, C., Assessment of the Influence of Different Cooling System Configurations on Engine Warm-Up, Emissions and Fuel Consumption, International Journal of Automotive Technology, vol. 9, no. 4, pp. 447–458, 2008.

[7] Luptowski, B. J., Arici, O., Johnson, J. H., and Parker, G. G. Development of the Enhanced Vehicle and Engine Cooling System Simulation and Application to Active Cooling Control, SAE paper 2005–01-0697, 2005. Available online at http://papers.sae.org/2005-01-0697

[8] Torregrosa, A. J., Olmeda, P., Degrauwe, B., and Reyes, M., A Concise Wall Temperature Model for DI Diesel Engines, Applied Thermal Engineering, vol. 26, no. 11–12, pp. 1320–1327, 2006.

[9] Shayler, P. J., Christian, S. J., and Ma, T., A Model for the Investigation of Temperature, Heat Flow and Friction Characteristics During Engine Warm-Up, SAE paper 931153, 1993. Available online at http://papers.sae.org/931153

[10] Taylor, C. F., and Toong, T. Y., Heat Transfer in Internal Combustion Engines, ASME paper 57-HT 17, 1957. Available online at http://www.asme.org/Publications

[11] Bohac, S. V., Baker, D. M., and Assanis, D. N., A Global Model for Steady State and Transient S.I. Engine Heat Transfer Studies, SAE Paper 960073, 1996. Available online at http://papers.sae.org/960073

[12] Annand, W. J. D., Heat Transfer in the Cylinders of Reciprocating Internal Combustion Engines, Proceedings of the Institution of Mechanical Engineers, vol. 177, pp. 973–990, 1963.

[13] Jarrier, L., Champoussin, J. C., Yu, R., and Gentile, D., Warm Up of a D.I. Diesel Engine: Experiment and Modelling, SAE Paper 2000–01-0299, 2000. Available online at http://papers.sae.org/2000-01-0299

[14] Charmantray, C., Champossin, J. C., and Yu, R., Coupling Nodal and Multi-Zone Combustion Models to Describe Thermal Diesel Engine

Behavior, SAE paper 2008–01-0845, 2008. Available online at http://papers.sae.org/2008-01-0845

[15] Esfahanian, V., Javaheri, A., and Ghaffarpour, M., Thermal Analysis of an SI Engine Piston Using Different Combustion Boundary Condition Treatments, Applied Thermal Engineering, vol. 26, pp. 277–287, 2006.

[16] Kubicki, M., Watson, H. C., Williams, J., and Stryker, P. C., Spatial and Temporal Temperature Distributions in a Spark Ignition Engine Piston at WOT, SAEpaper 2007–01-1436, 2007. Available online at http://papers.sae.org/2007-01-1436

[17] Incropera, F., and Dewitt, D.P., Fundamentals of Heat and Mass Transfer, 4th ed., John Wiley & Sons, New York, 1996.

[18] Schubert, C.,Wimmer, A., and Chmela, F., Advanced Heat TransferModel for CI Engines, SAE paper 2005–01-0695, 2005. Available online at http://papers.sae.org/2005-01-0695

[19] Woschni, G. A., Universally Applicable Equation for the Instantaneous Heat Transfer Coefficient in the Internal Combustion Engine, SAE Paper 670931, 1967. Available online at http://papers.sae.org/670931

[20] Benajes, J., Torregrosa, A. J., and Reyes, M., Heat Transfer Model for IC Engine Exhaust Manifolds, Proc. of the Eurotherm Seminar, IMFT Toulouse, France, vol. 15, pp. 189–194, 1991.

[21] Payri, F., Molina, S., Mart´ın, J., and Armas, O., Influence of Measurement Errors and Estimated Parameters on Combustion Diagnosis, Applied Thermal Engineering, 26 (2–3), 226–236, 2006.

[22] Dittus, F. W., and Boelter, L. M. K., Heat-Transfer in Automobile Radiators of the Tubular Type, University of California Publications in Engineering, vol. 2, pp. 443–461, 1930.

[23] Robinson, K., Hawley, J. G., Hammond, G. P., and Owen, N. J., Convective Coolant Heat Transfer in Internal Combustion Engines, Proceedings of the Institution of Mechanical Engineers, vol. 217, part D, Journal of Automobile Engineering, pp. 136–146, 2003.

[24] Chang, S.W.; Su, L. M.; Yang, T. L., et al., Enhanced Heat Transfer of Shaker-Bored Piston Cooling Channel With Twisted Tape Insert, Heat Transfer Engineering, vol. 28, no. 4, pp. 321–334, 2007.

[25] Agarwal, A. K., and Varghese, M. B., Numerical Investigations of Piston Cooling Oil Jet in Heavy Duty Diesel Engines, International Journal of Engine Research, vol. 7, pp. 411–421, 2006.

[26] Torregrosa, A. J., Broatch, A., Olmeda, P., and Martin, J., A Contribution to Film Coefficient Estimation in Piston Cooling Galleries, Experimental Thermal and Fluid Science, vol. 34, no. 2, pp. 142–151, 2010.

[27] Lee, C., Chiang, K., Chen, W., and Chen, R., Design and Analysis of Gasket Sealing of Cylinder Head Under Engine Operation Conditions, Finite Elements in Analysis and Design, vol. 41, pp. 1160–1174, 2005.

[28] Degrauwe, B., Contribution to the Thermal Management of DI Diesel Engines, Ph.D. thesis, Universidad Politécnica de Valencia, Spain, 2006.

[29] Stone, R., Introduction to Internal Combustion Engines, 3rd ed., SAE International, Warrendale, PA, 1999.

[30] Klein, M., Eriksson, L., and Aslund, J., Compression Ratio Estimation Based on Cylinder Pressure Data, Control Engineering Practice, vol. 14, no. 3, pp. 197–211, 2006.

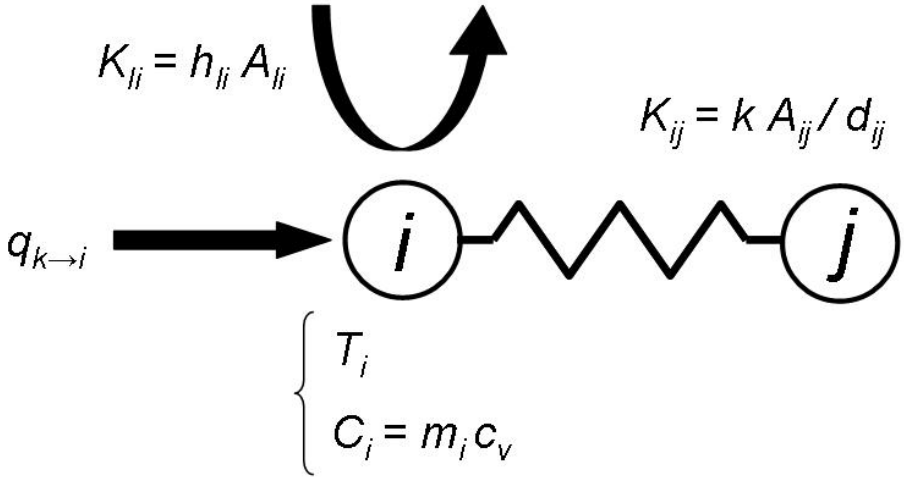

Figure 1. Node of a thermal network

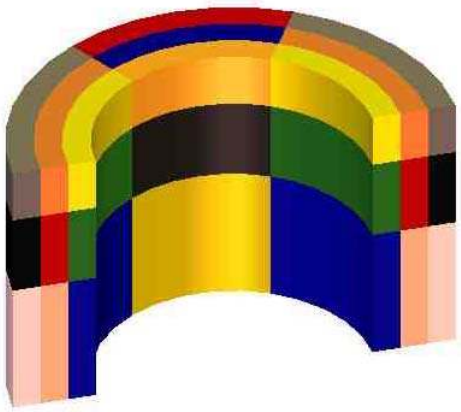

Figure 2. Cylinder liner discretization

Figure 3. Expanded view of the piston

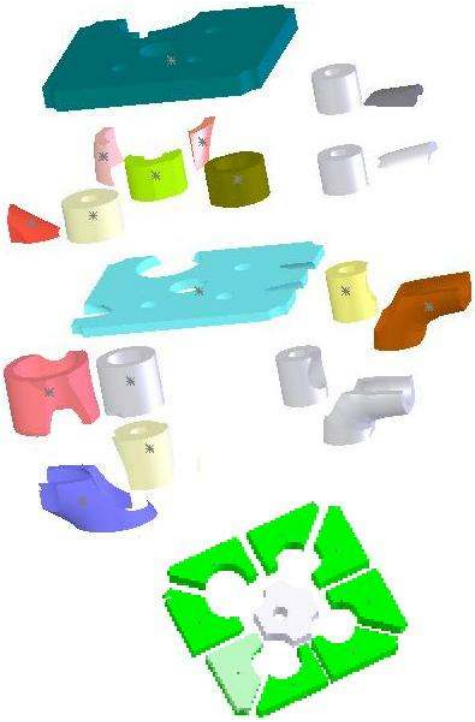

Figure 4. Cylinder head discretization

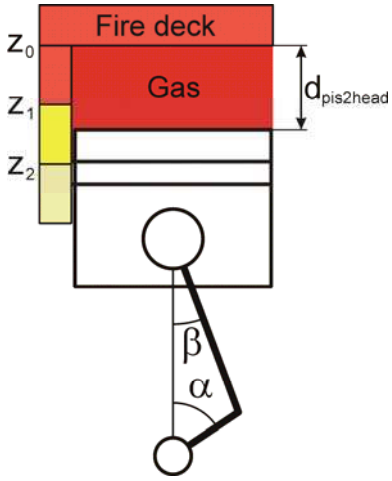

Figure 5. Cylinder gas – liner interaction.

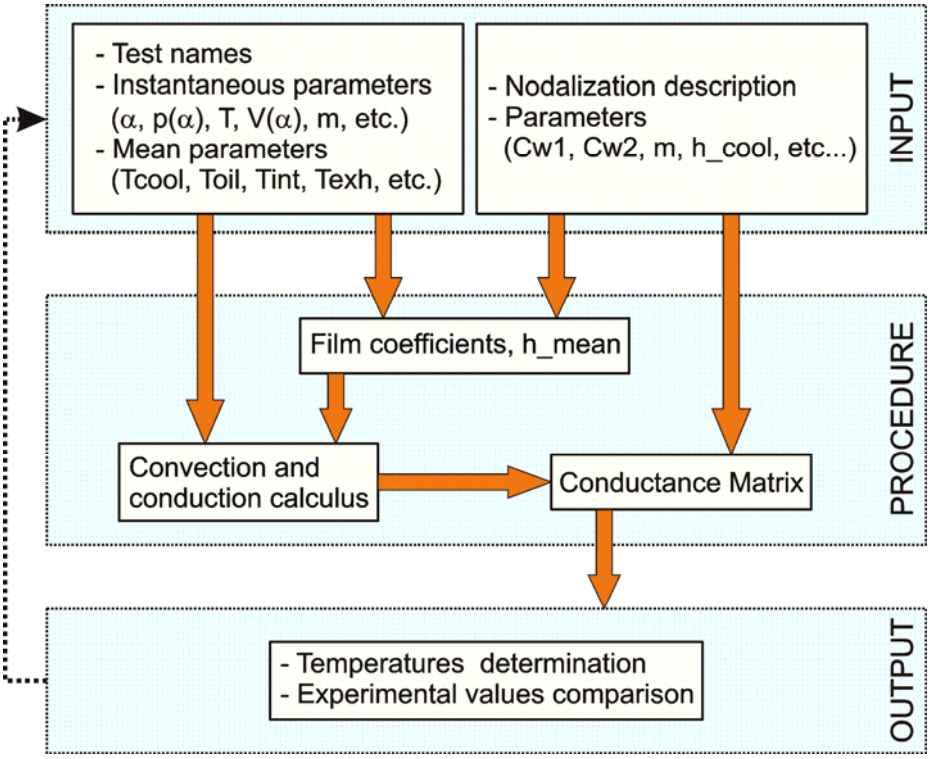

Figure 6. Structure of the computational program used for the model.

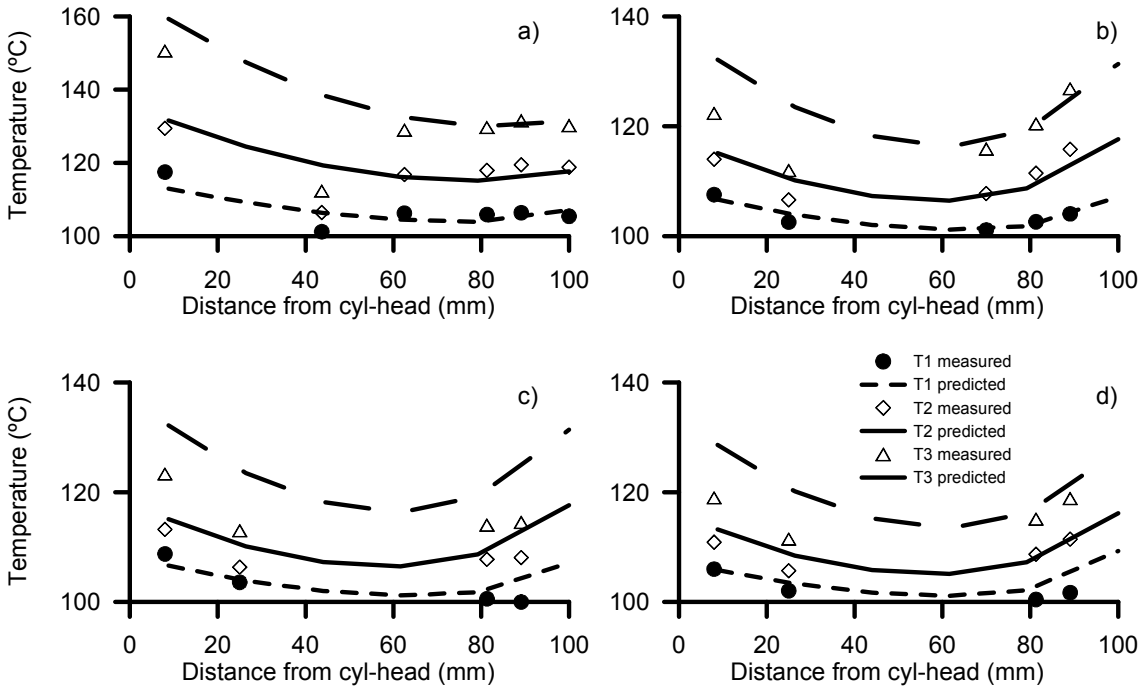

Figure 7. Predicted and measured temperature distributions in the liner at various axial locations: a) between cylinders side, b) intake side, c) exhaust side, d) clutch side.

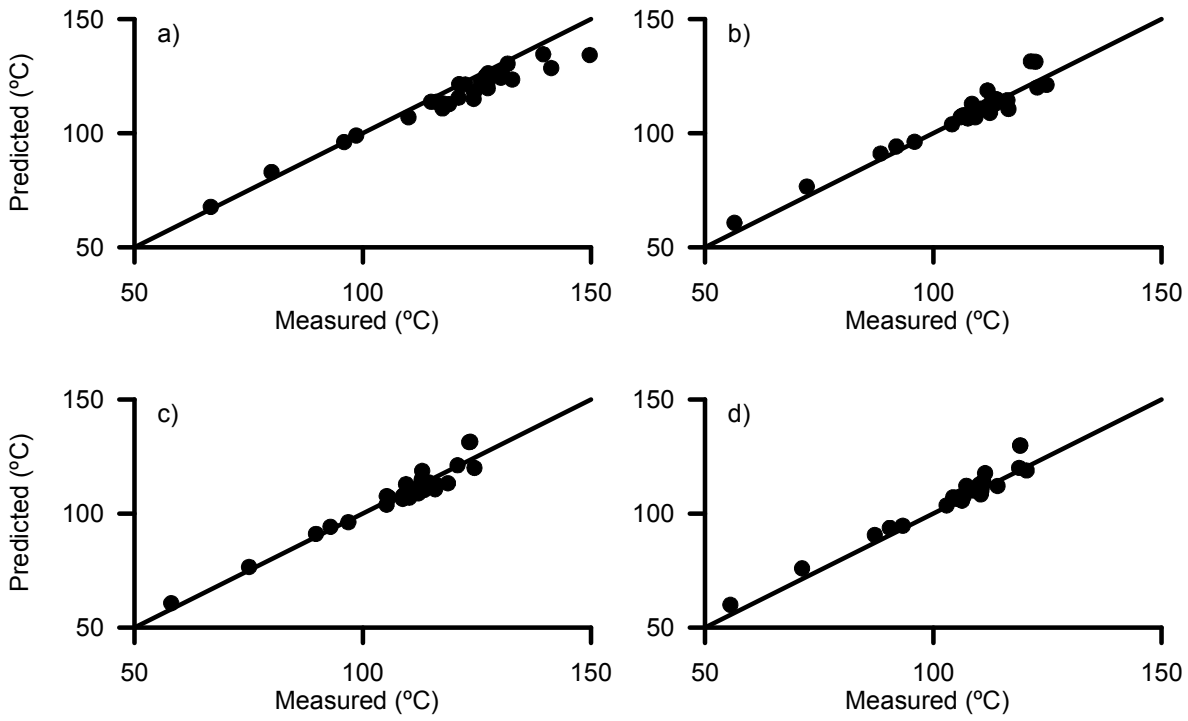

Figure 8. Predicted and measured temperatures in the liner nodes: a) between cylinders side, b) intake side, c) exhaust side, d) clutch side.

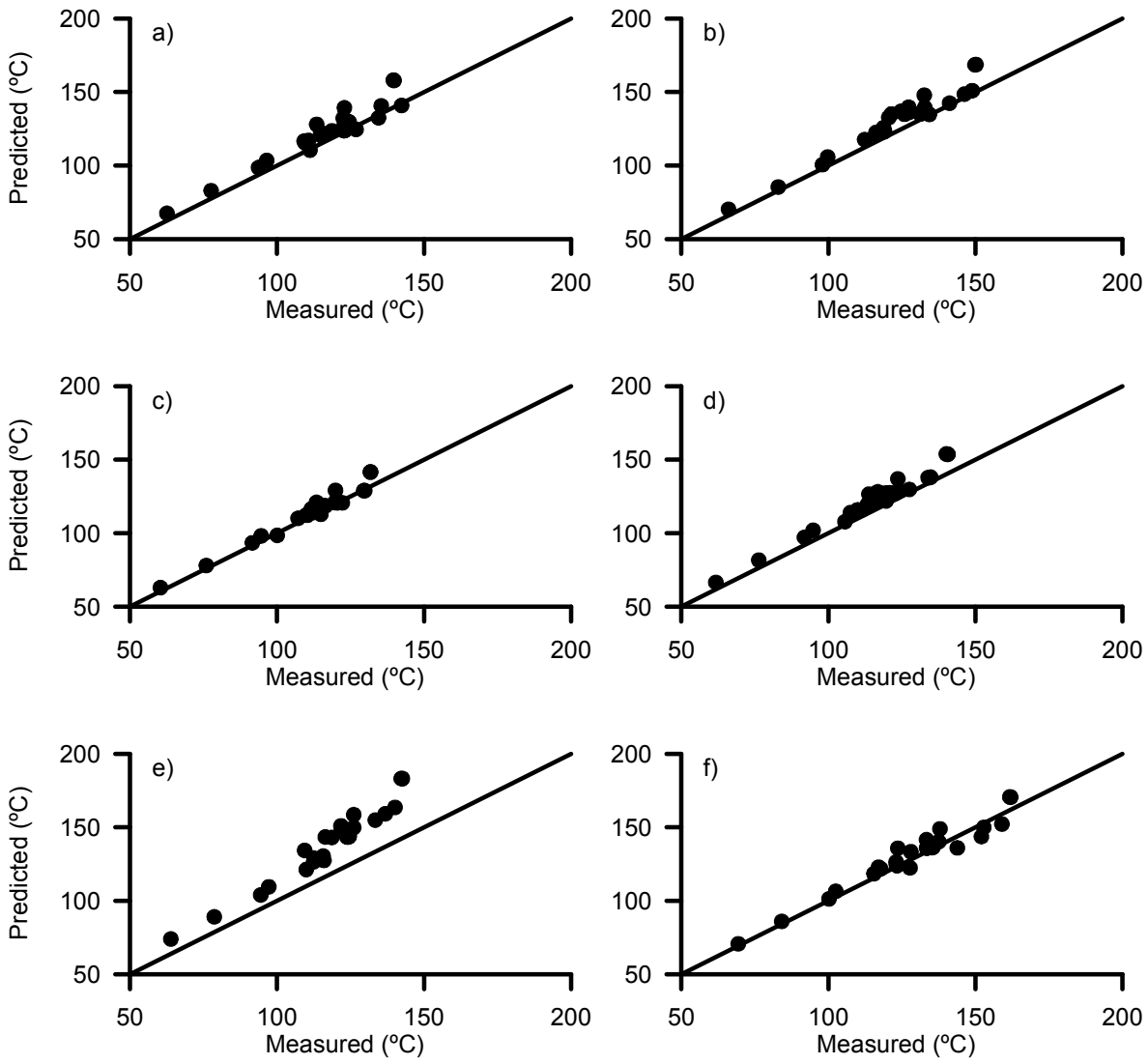

Figure 9. Predicted and measured temperatures in the cylinder head nodes: a) Exhaust valve seat, b) Between exhaust and intake valves, c) Intake valve seat, d) Between cylinders, e) injector hole, f) Between exhaust valves

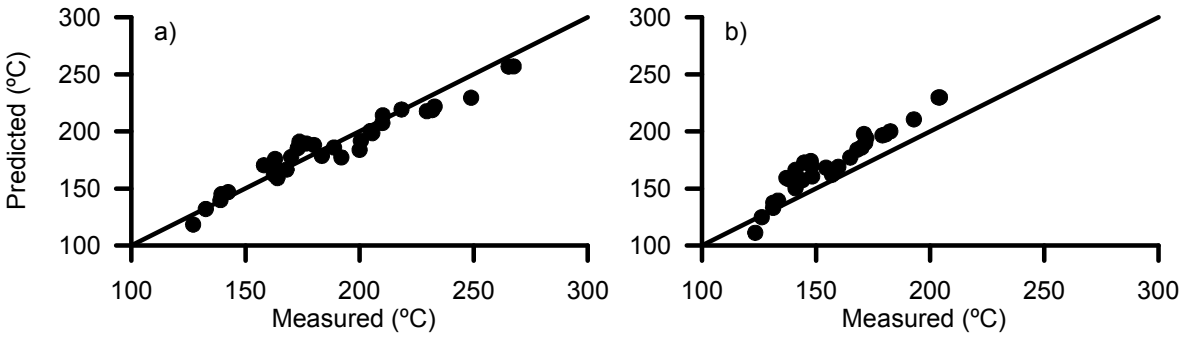

Figure 10. Predicted and measured temperatures in the piston nodes: a) Bowl rim, b) Bowl bottom

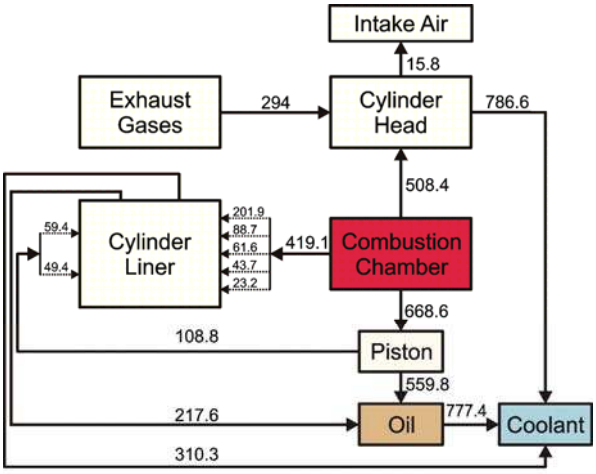

Figure 11. Heat exchange between the nodes of the model (heat fluxes in watts).

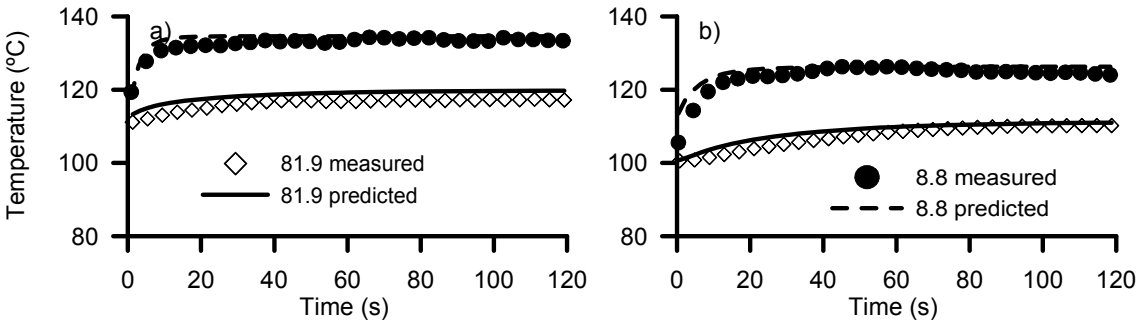

Figure 12. Transient temperatures for a couple of extreme liner nodes under two transient processes a) 4500 rpm (2-8 bar), b) 1000 rpm (3-10 bar)

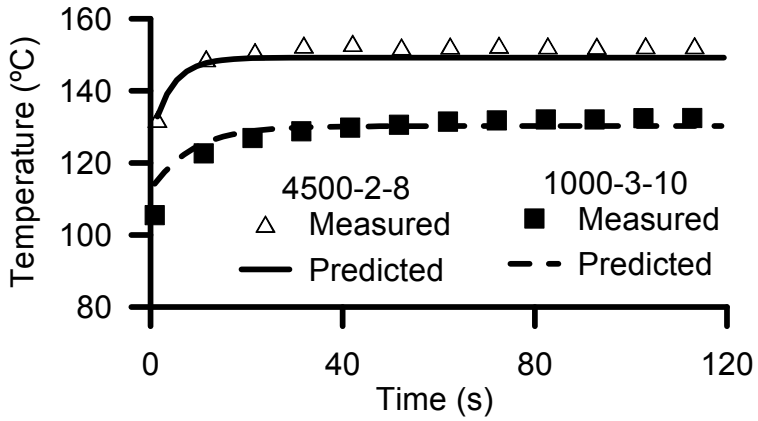

Figure 13. Transient temperatures for the exhaust valve seat, under two engine transient processes: 4500 rpm (2-8 bar) and 1000 rpm (3-10 bar).

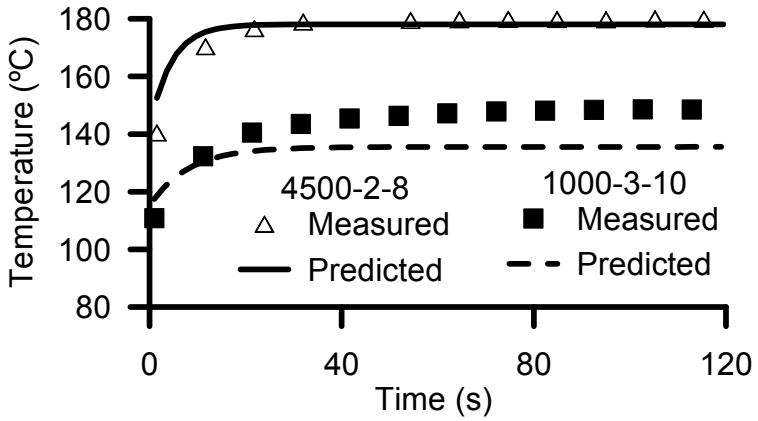

Figure 14. Transient temperatures for the node between exhaust valves under two engine transient processes: 4500 rpm (2-8 bar) and 1000 rpm (3-10 bar).

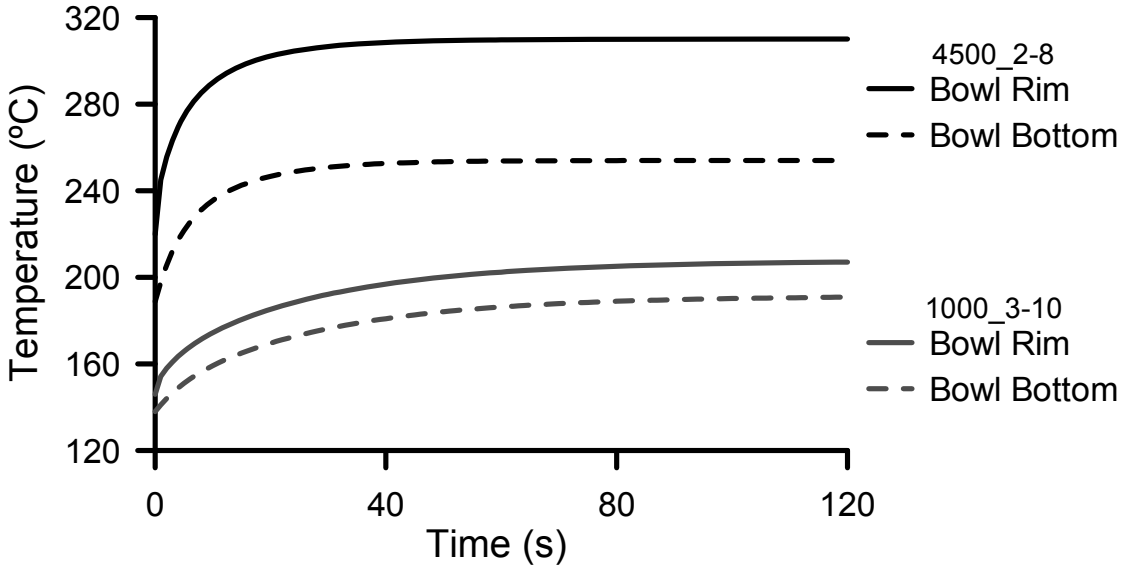

Figure 15. Predicted transient temperatures for the piston nodes under two step transient processes: 4500 rpm (2-8 bar) and 1000 rpm (3-10 bar).

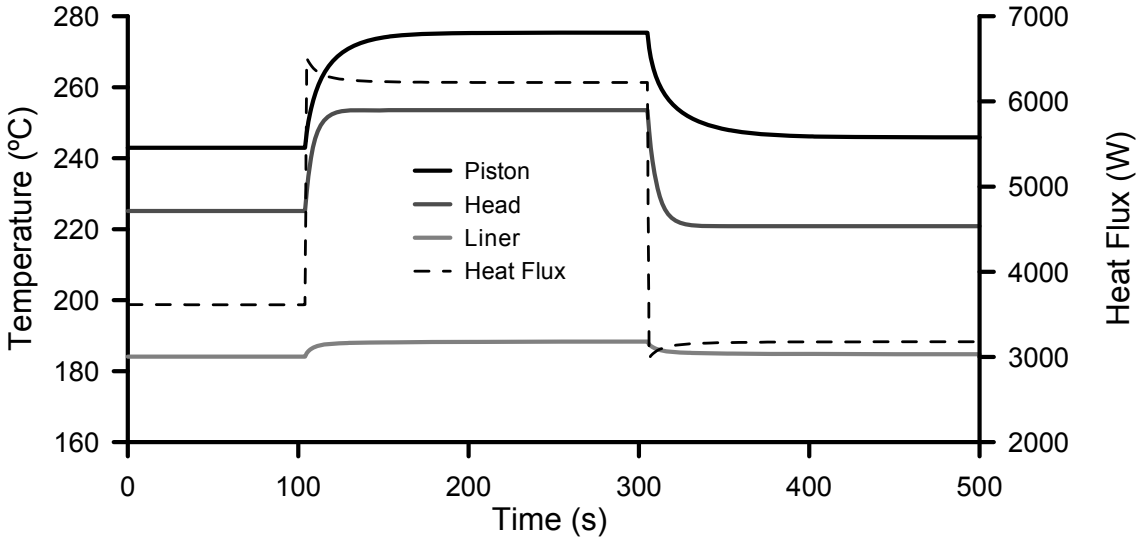

Figure 16. Transient heat flux evolution as the engine is subjected to a stair-step schedule of operating conditions.

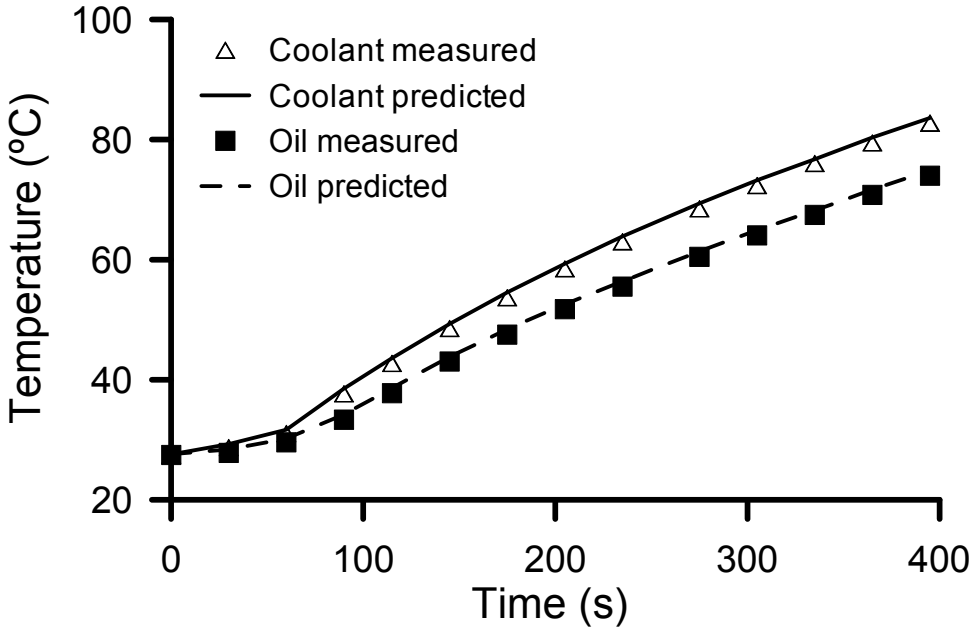

Figure 17. Oil and coolant temperatures (predicted and measured) for a warm-up in the second engine.

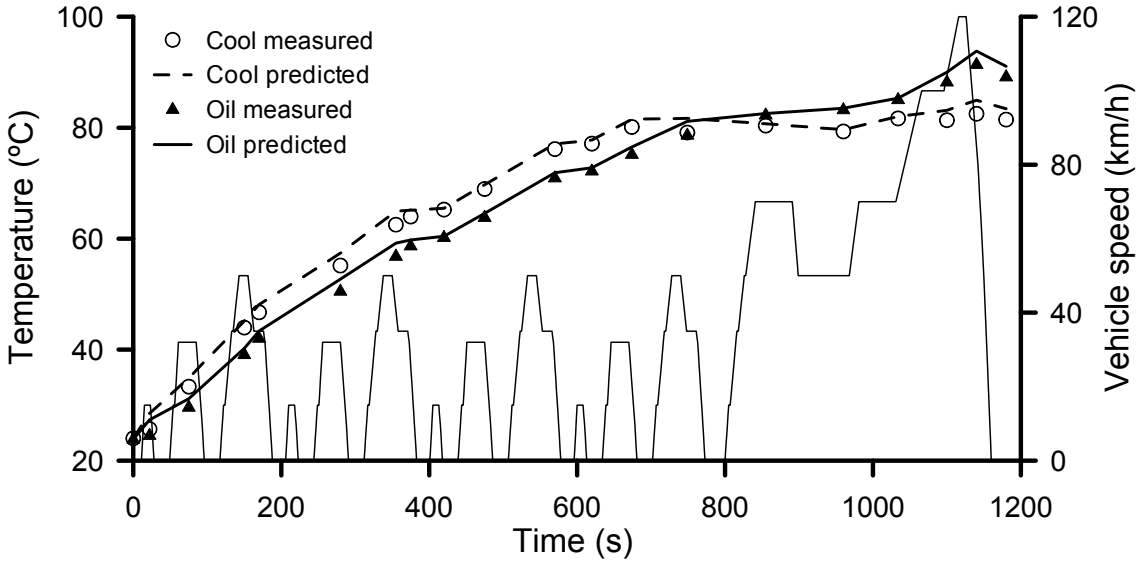

Figure 18. Oil and coolant temperature evolution in a NEDC. Comparison between experimental and model results.

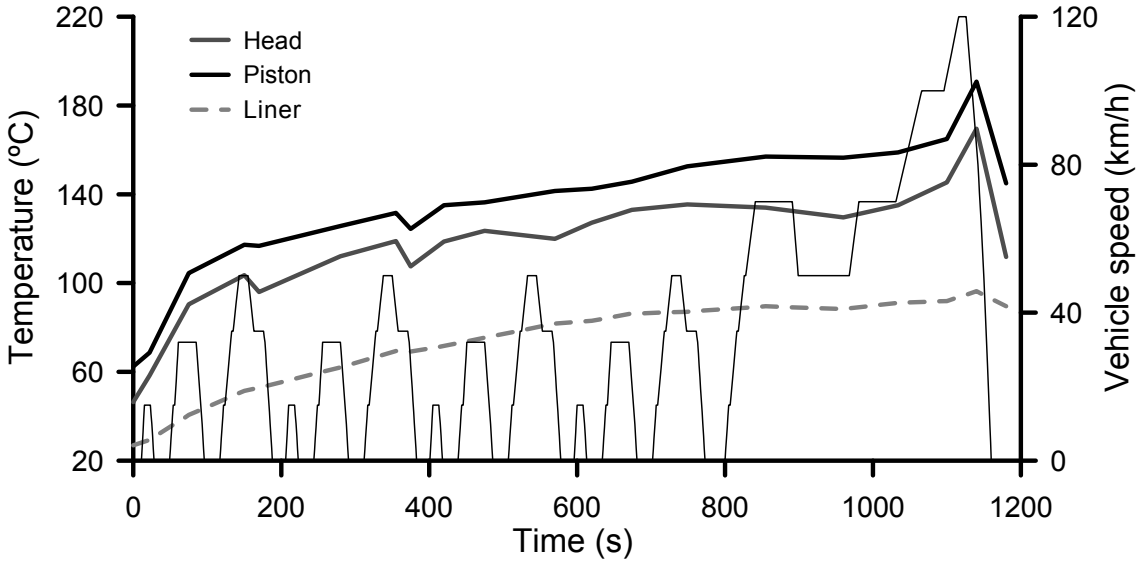

Figure 19. Predicted material temperature evolution in a NEDC.

Table 1. Engine main characteristics

Stroke [mm]	80
Bore [mm]	75
Maximum bmep [bar]	19.6
Nominal speed [rpm]	2000

Table 2. Tests used to adjust the model.

Parameter	Range of variation	Conditions (speed and load)
Load (bar)	4.92 – 13.23	1500 rpm
	3.10 – 11.56	2000 rpm
	2.17 – 11.93	2500 rpm
	3.08 – 11.75	3000 rpm
	2.63 – 14.41	3500 rpm
Coolant Temperature (ºC)	47 – 97	1520 rpm; 2.51 bar
	81 – 97	1430 rpm; 5.14 bar
	65 – 97	2380 rpm; 10.08 bar
Oil Temperature (ºC)	75 – 105	2000 rpm; 7.25 bar
	80 – 107	3000 rpm; 6.50 bar
	85 – 115	4000 rpm; 3.40 bar
Intake manifold pressure (bar)	1.05 – 1.8	2000 rpm; 7.40 bar mep

Table 3. Optimized values of conductance parameters used in the model.

Parameter	Equation	Optimized value
Constant of correlation piston oil (b_7)	22	721.4
Reynolds exponent of correlation piston -oil (b_5)	22	0.687
Heat transfer coefficient between liner and oil ($h_{lin-oil}$)	22	864.9
Conductance between piston and liner ($K_{pis-lin}$)	23	3.876

Table 4. Summary of tests for unsteady conditions.

Parameter	Range of variation	Conditions
Load (bar)	3.3 – 10.7 - 3.3	1000 rpm
	3.9 – 16.9 – 3.9	1500 rpm
	6.5 – 18.8 – 6.5	2000 rpm
	3.3 – 12.0 -3.3	
	4.2 – 12.6 – 4.2	2500 rpm
	4.4 – 12.8 – 4.4	3000 rpm
	1.7 – 5.4 – 1.7	
	4.2 – 12.2 – 4.2	3500 rpm
	2.6 – 8.6 -2.6	4000 rpm
	2.4 – 8.8 - 2.4	4500 rpm
Speed (rpm)	1078 – 3013 - 1078	4 bar
	1090 – 2710 -1090	8 bar
	1040 – 4000 – 1040	8 bar

Table 5. Second engine main characteristics

Stroke [mm]	88
Bore [mm]	85
Maximum bmep [bar]	19.4
Nominal speed [rpm]	1800

Brief biographical notes about the authors:

Antonio J. Torregrosa is Professor in the Department of thermal engines at the Universidad Politécnica de Valencia (Spain) since 2002 He obtained his PhD at the same University in 1993. He has been head of Diesel engine's thermal management Line in CMT-Motores Térmicos since 2003.

Pablo Olmeda received the degree of Mechanical Engineering in the Universidad Politécnica de Valencia in 1998 and his PhD at the same University in 2003. He is Associate Professor since 2009 in the Department of Thermal Engines. His main research activities focused on Diesel engine's thermal management.

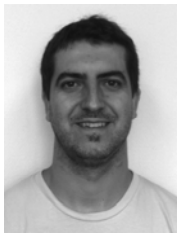

Jaime Martín received the degree of Mechanical Engineering in the Universidad Politécnica de Valencia in 2001 and his PhD at the same University in 2007. He has been an Assistant Professor since 2005 in the Department of Thermal Engines. His main research activities focused on combustion diagnosis in Diesel engines starting from the in-cylinder pressure and thermodynamic modelling.

Carlos Romero received the degree of Mechanical Engineering in the Belarusian Polytechnic Institute in 1986 and his PhD in the Universidad Politécnica de Valencia in 2009. He is an Assistant Professor since 2003 at the School of Mechanical Technology in the Universidad Tecnológica de Pereira, Colombia. His main research activities focus on alternative combustion engine modelling and instrumentation.